Supplementary data

Figure S1. XPS spectra for the Ag@PBC 300 a) Ag@PBC survey, b) C1s, O1s and d) Ag3d.

Figure S2. XPS spectra for the Ag@PBC 400 a) Ag@PBC survey, b) C1s, O1s and d) Ag3d.

Figure S3. XPS spectra for the Ag@PBC 600 a) Ag@PBC survey, b) C1s, O1s and d) Ag3d.

Figure S4. EDS spectra and elemental composition of (a) PBC and (b) Ag@PBC composite.

Figure S5. TEM images of Ag@PBC 300 composite at different magnifications (a–c) and the SAED pattern (d).

Figure S6. TEM images of Ag@PBC 400 composite at different magnifications (a–c) and the SAED pattern (d).

Figure S7. TEM images of Ag@PBC 600 composite at different magnifications (a–c) and the SAED pattern (d).

Figure S8. N_2 adsorption-desorption isotherms biochar a) PBC 300, b) PBC 600 and composites c) Ag@PBC 300 & d) Ag@PBC 600.

Figure S9. Time-dependent UV–Vis spectra showing the catalytic reduction of 4-nitrophenol to 4-aminophenol using Ag@PBC 300 at different molar ratios of 4-NP:$NaBH_4$: (a) 1:5, (b) 1:10, (c) 1:25, (d) 1:50, (e) 1:75, and (f) 1:100.

Figure S10. Time-dependent UV–Vis spectra showing the catalytic reduction of 4-nitrophenol to 4-aminophenol using Ag@PBC 400 at different molar ratios of 4-NP:$NaBH_4$: (a) 1:5, (b) 1:10, (c) 1:25, (d) 1:50, (e) 1:75, and (f) 1:100.

Figure S11. Time-dependent UV–Vis spectra showing the catalytic reduction of 4-nitrophenol to 4-aminophenol using Ag@PBC 500 at different molar ratios of 4-NP:$NaBH_4$: (a) 1:5, (b) 1:10, (c) 1:25, (d) 1:50, (e) 1:75, and (f) 1:100.

Figure S12. Time-dependent UV–Vis spectra showing the catalytic reduction of 4-nitrophenol to 4-aminophenol using Ag@PBC 600 at different molar ratios of 4-NP:$NaBH_4$: (a) 1:5, (b) 1:10, (c) 1:25, (d) 1:50, (e) 1:75, and (f) 1:100.

Figure S13. Time-dependent of absorbance showing the reduction of CR and MO at different concentrations 25ppm (a and d), 50ppm (b and e) and 100ppm (c and f) catalyzed by Ag@PBC 300.

Figure S14. Time-dependent of absorbance showing the reduction of CR and MO at different concentrations 25ppm (a and d), 50ppm (b and e) and 100ppm (c and f) catalyzed by Ag@PBC 400.

Figure S15. Time-dependent of absorbance showing the reduction of CR and MO at different concentrations 25ppm (a and d), 50ppm (b and e) and 100ppm (c and f) catalyzed by Ag@PBC 600.

Figure S16. Reusability of Ag@PBC catalysts over 10 cycles.

Figure S17. FTIR spectra of the Ag@PBC composites after 10^{th} catalytic cycles.

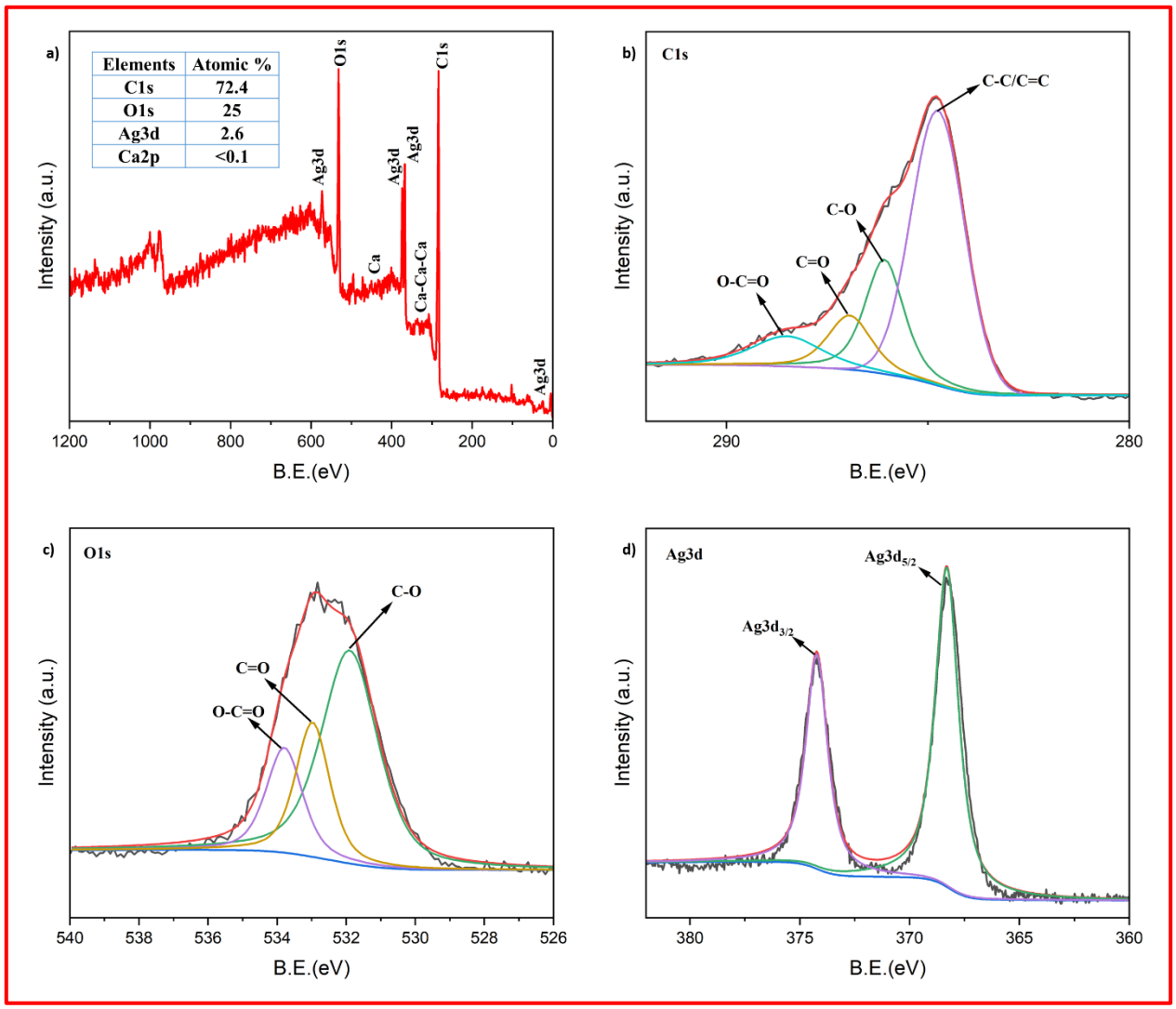

Figure S1. XPS spectra for the Ag@PBC 300 a) Ag@PBC survey, b) C1s, O1s and d) Ag3d.

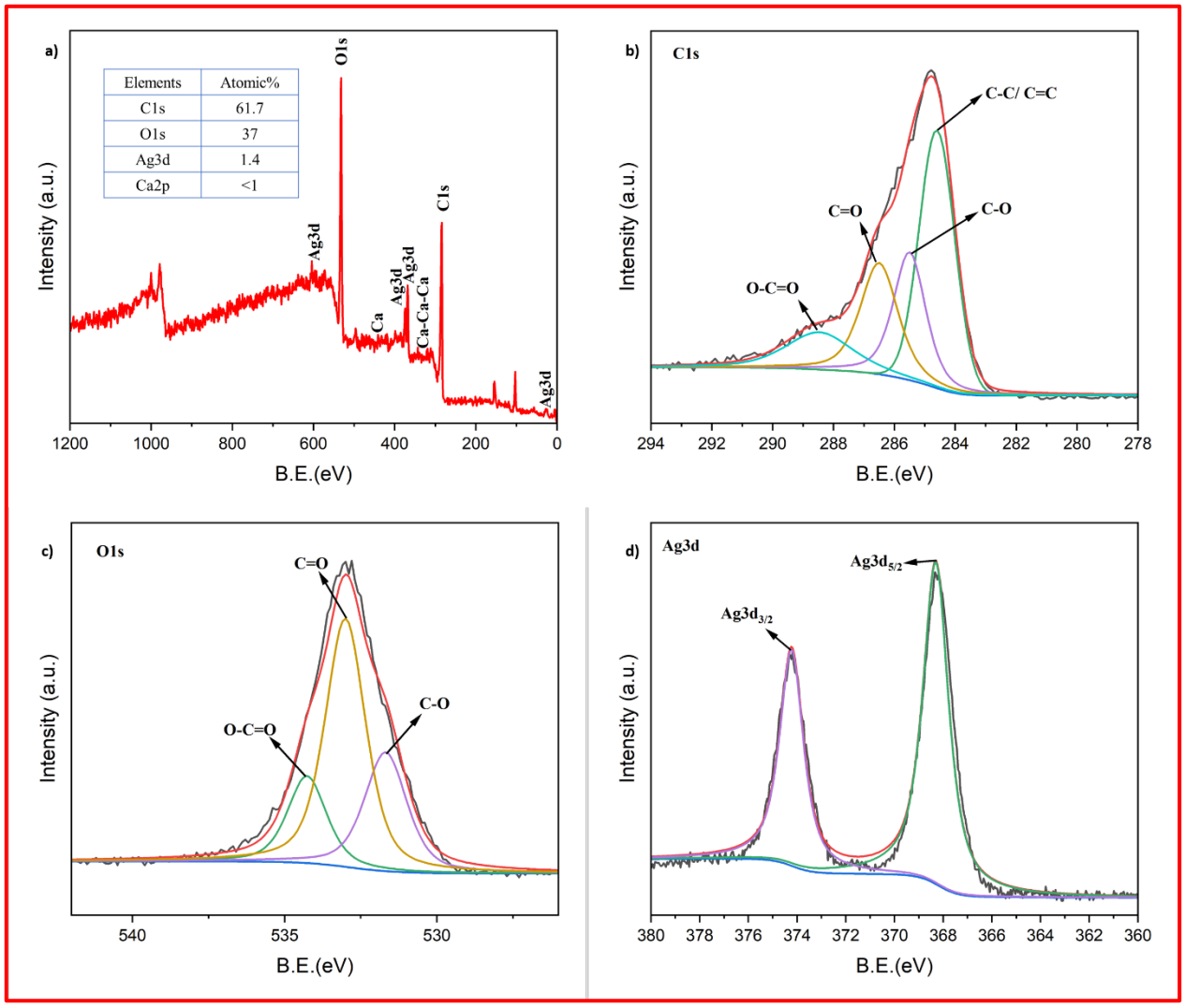

Figure S2. XPS spectra for the Ag@PBC 400 a) Ag@PBC survey, b) C1s, O1s and d) Ag3d.

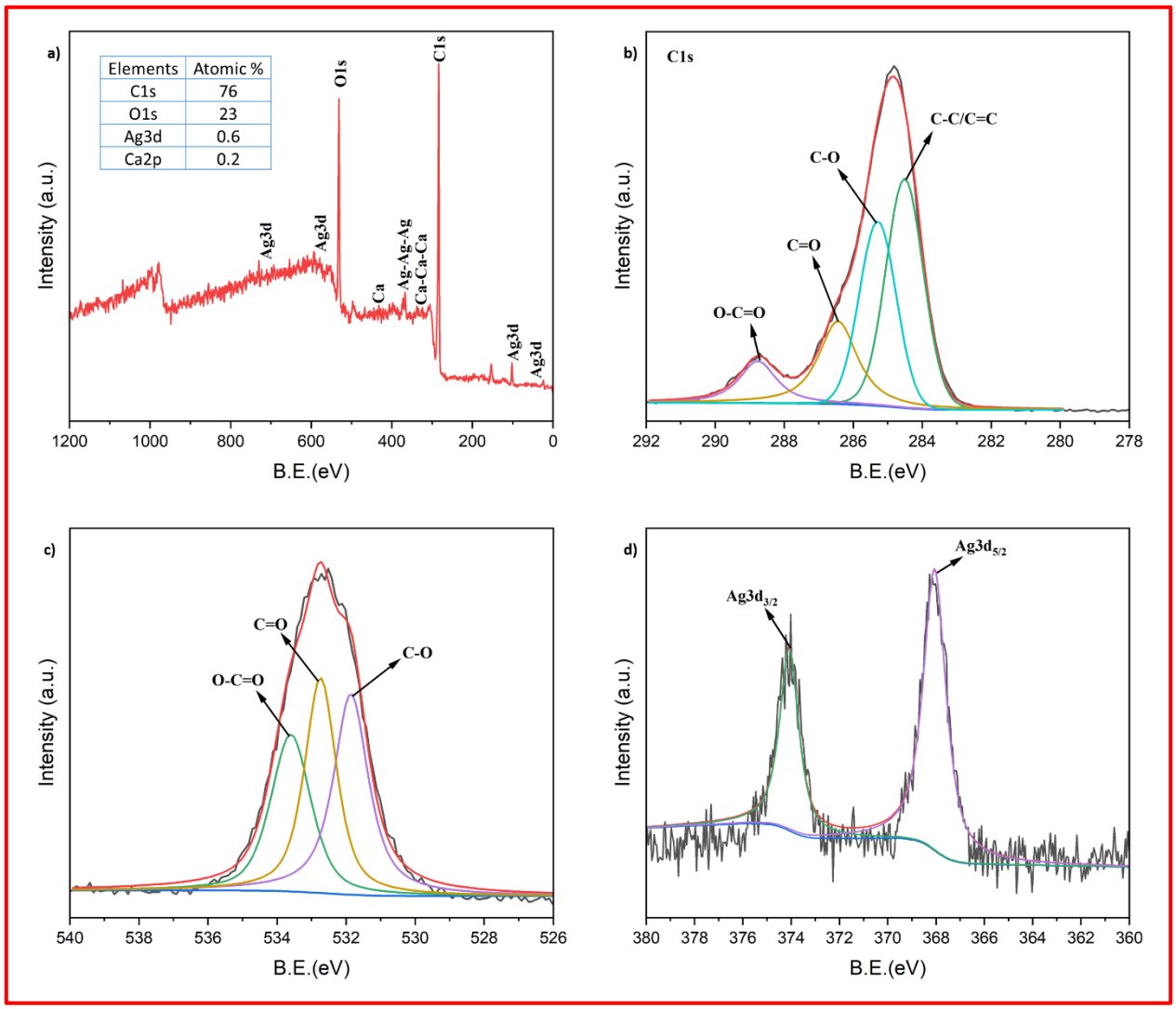

Figure S3. XPS spectra for the Ag@PBC 600 a) Ag@PBC survey, b) C1s, O1s and d) Ag3d.

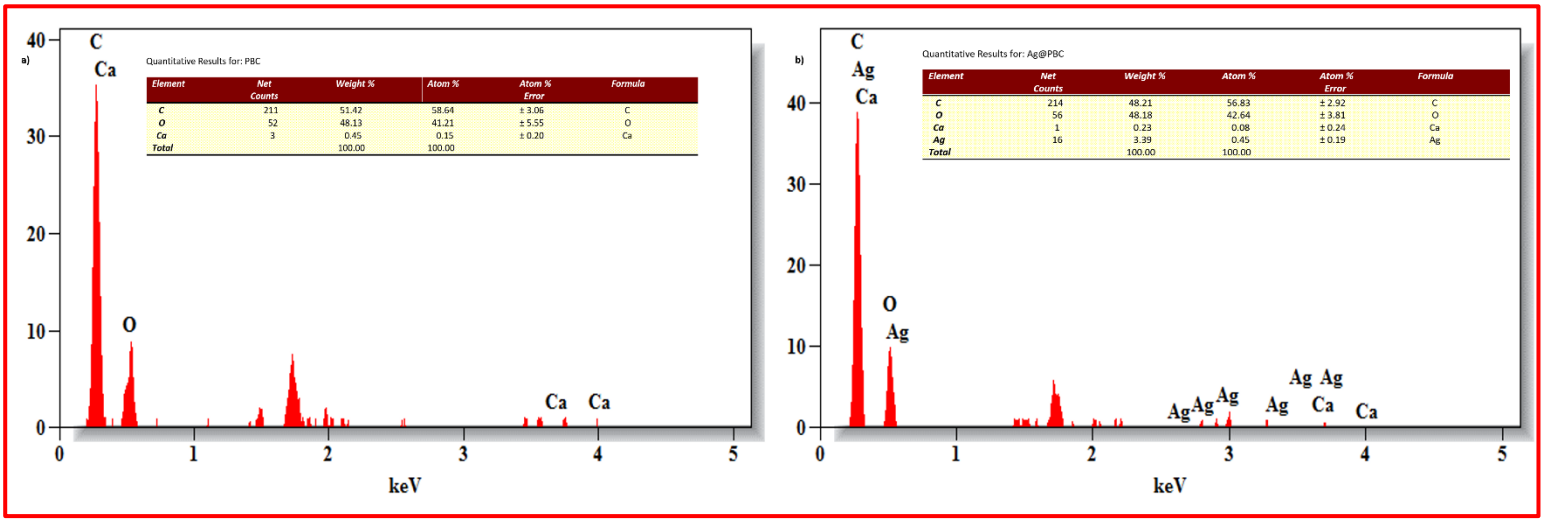

Figure S4. EDS spectra and elemental composition of (a) PBC and (b) Ag@PBC composite.

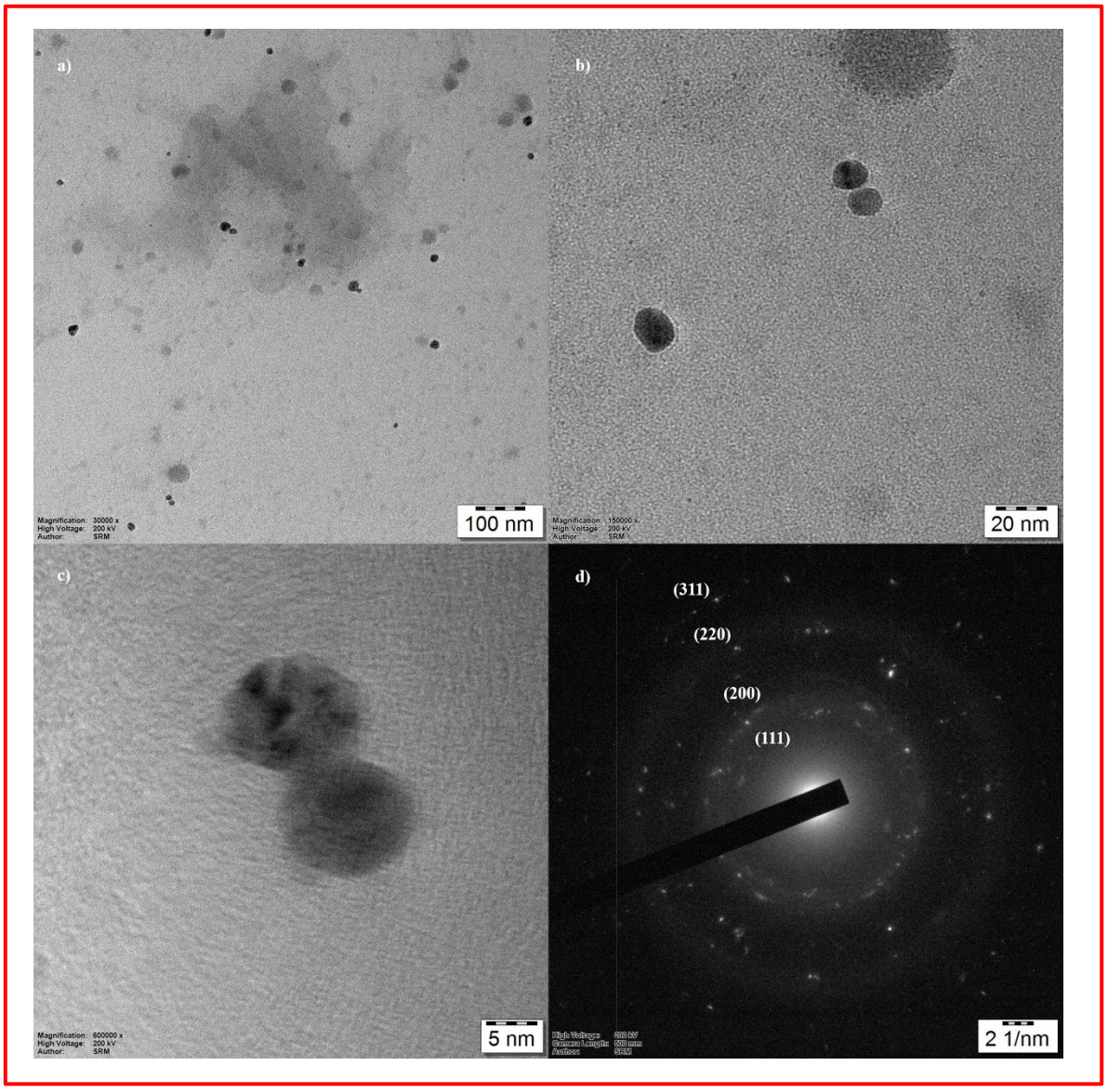

Figure S5. TEM images of Ag@PBC 300 composite at different magnifications (a–c) and the SAED pattern (d).

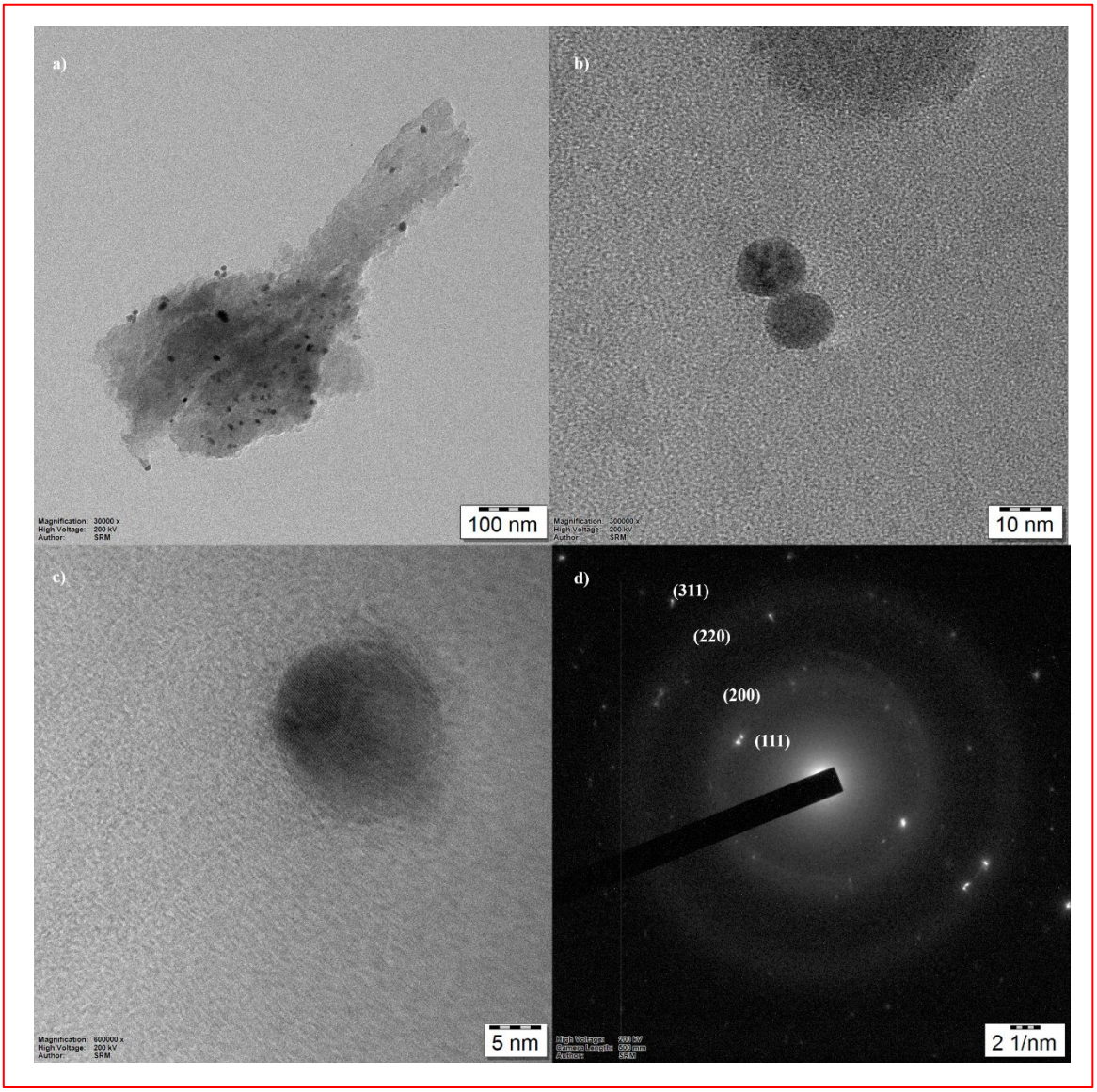

Figure S6. TEM images of Ag@PBC 400 composite at different magnifications (a–c) and the SAED pattern (d).

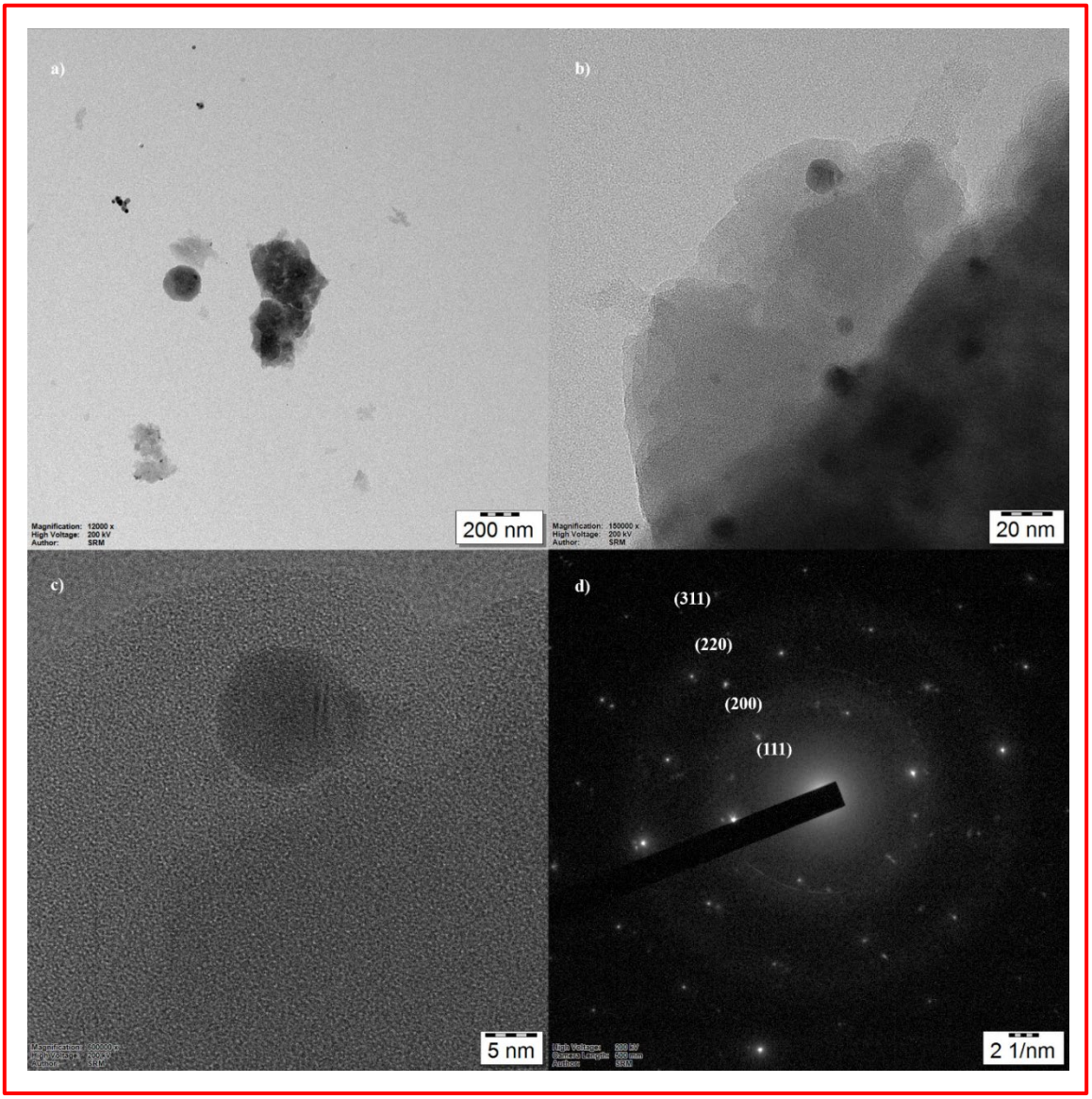

Figure S7.TEM images of Ag@PBC 600 composite at different magnifications (a–c) and the SAED pattern (d).

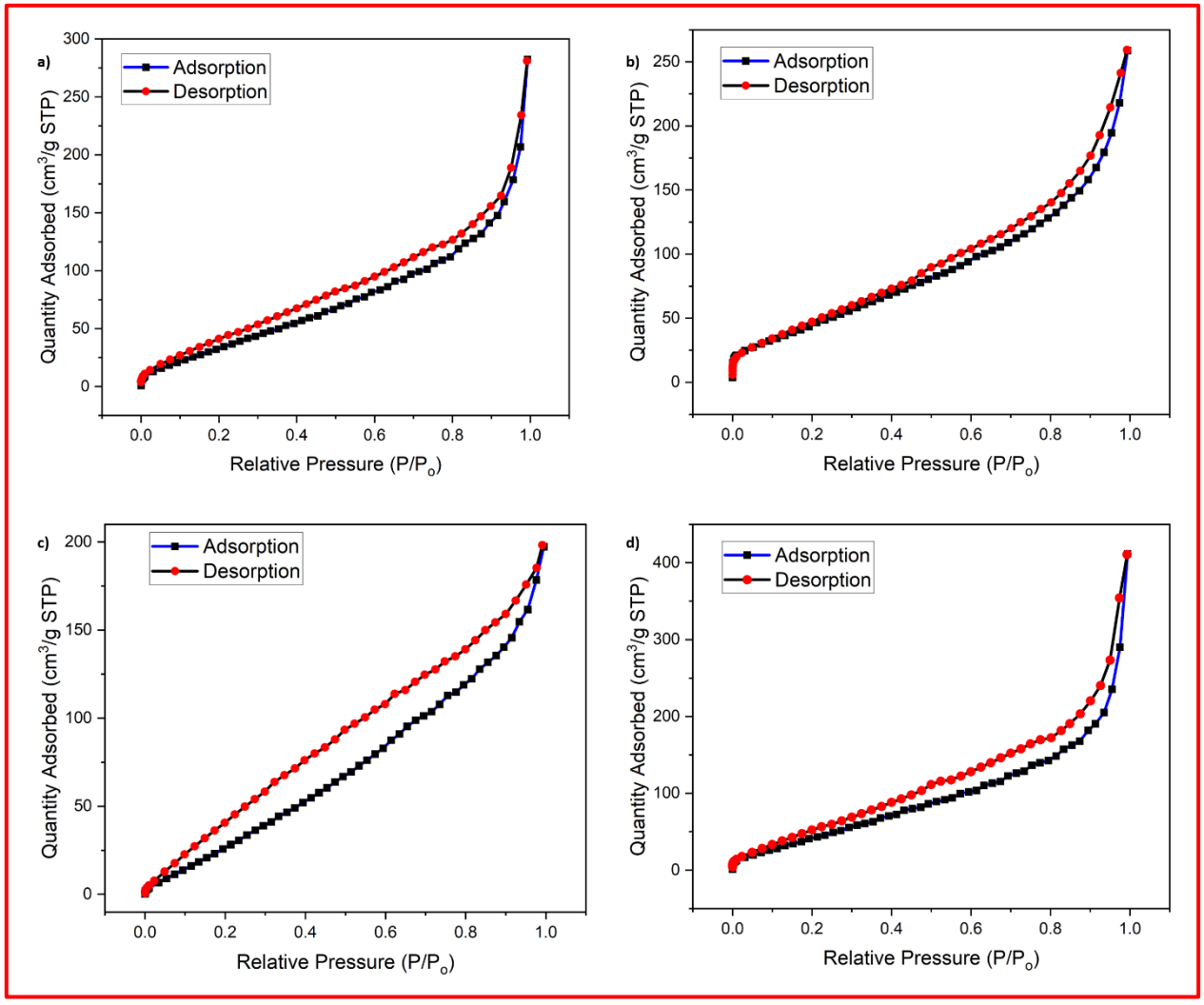

Figure S8. N_2 adsorption-desorption isotherms biochar a) PBC 300, b) PBC 600 and composites c) Ag@PBC 300 & d) Ag@PBC 600

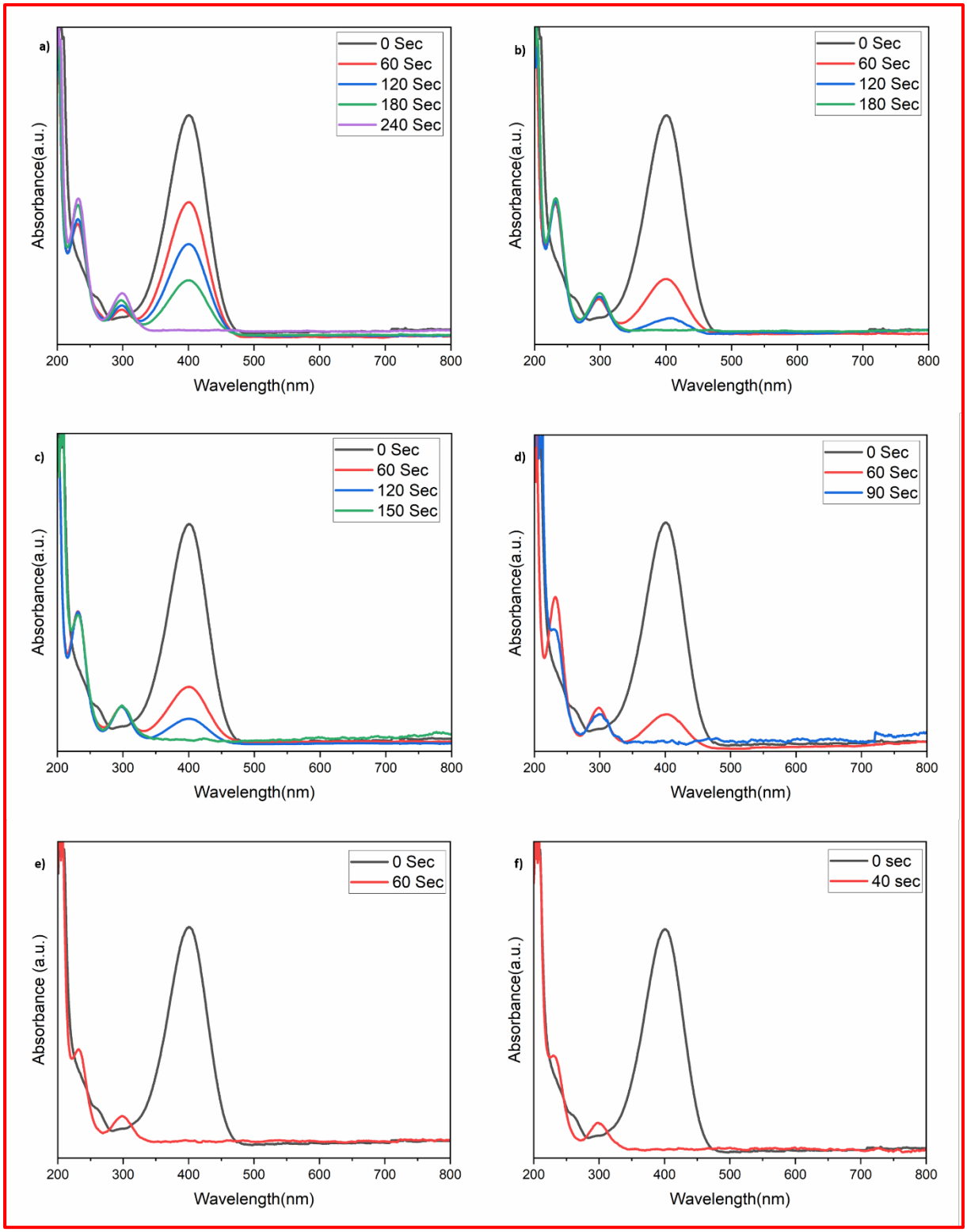

Figure S9. Time-dependent UV–Vis spectra showing the catalytic reduction of 4-nitrophenol to 4-aminophenol using Ag@PBC 300 at different molar ratios of 4-NP:$NaBH_4$: (a) 1:5, (b) 1:10, (c) 1:25, (d) 1:50, (e) 1:75, and (f) 1:100.

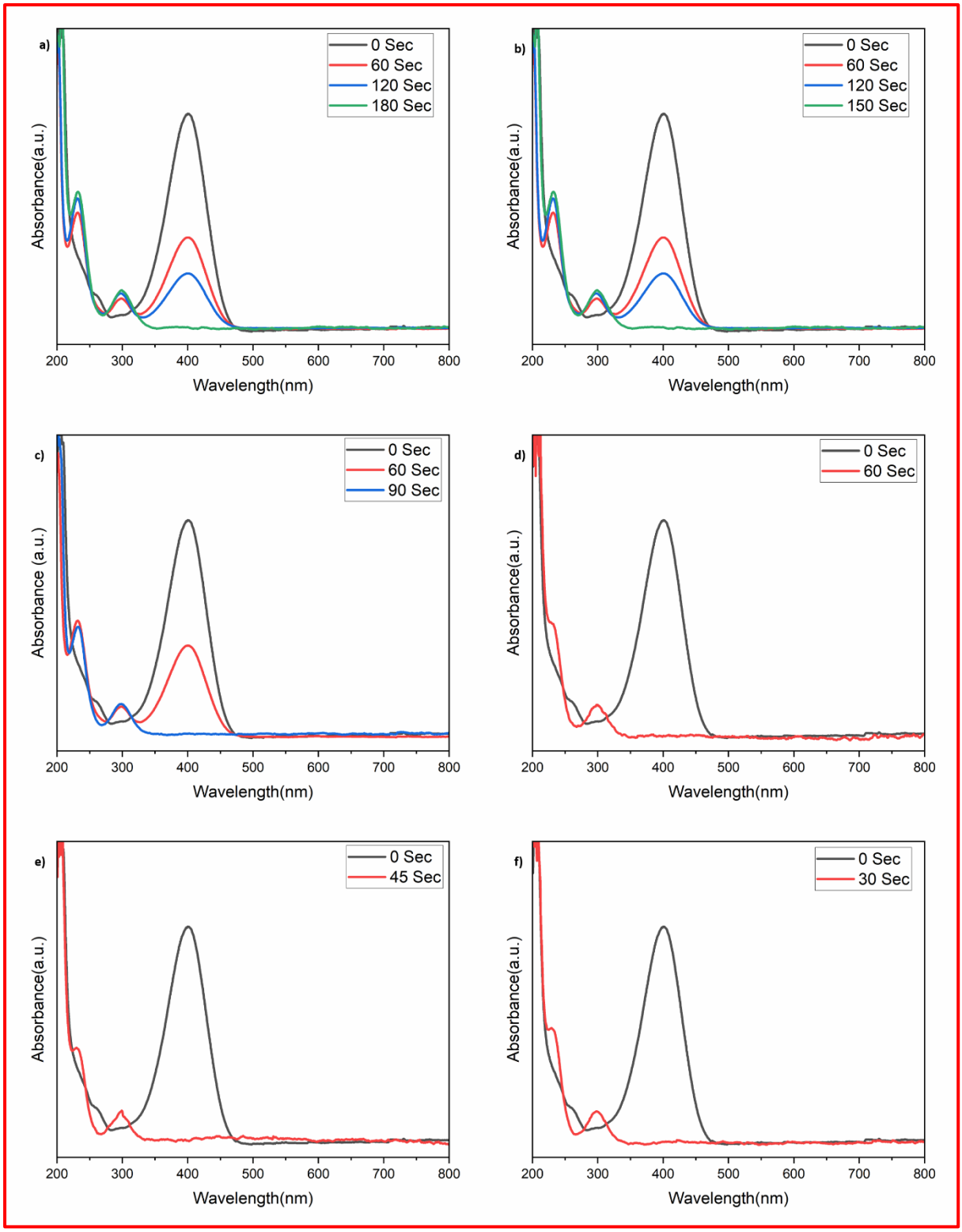

Figure S10. Time-dependent UV–Vis spectra showing the catalytic reduction of 4-nitrophenol to 4-aminophenol using Ag@PBC 400 at different molar ratios of 4-NP:$NaBH_4$: (a) 1:5, (b) 1:10, (c) 1:25, (d) 1:50, (e) 1:75, and (f) 1:100.

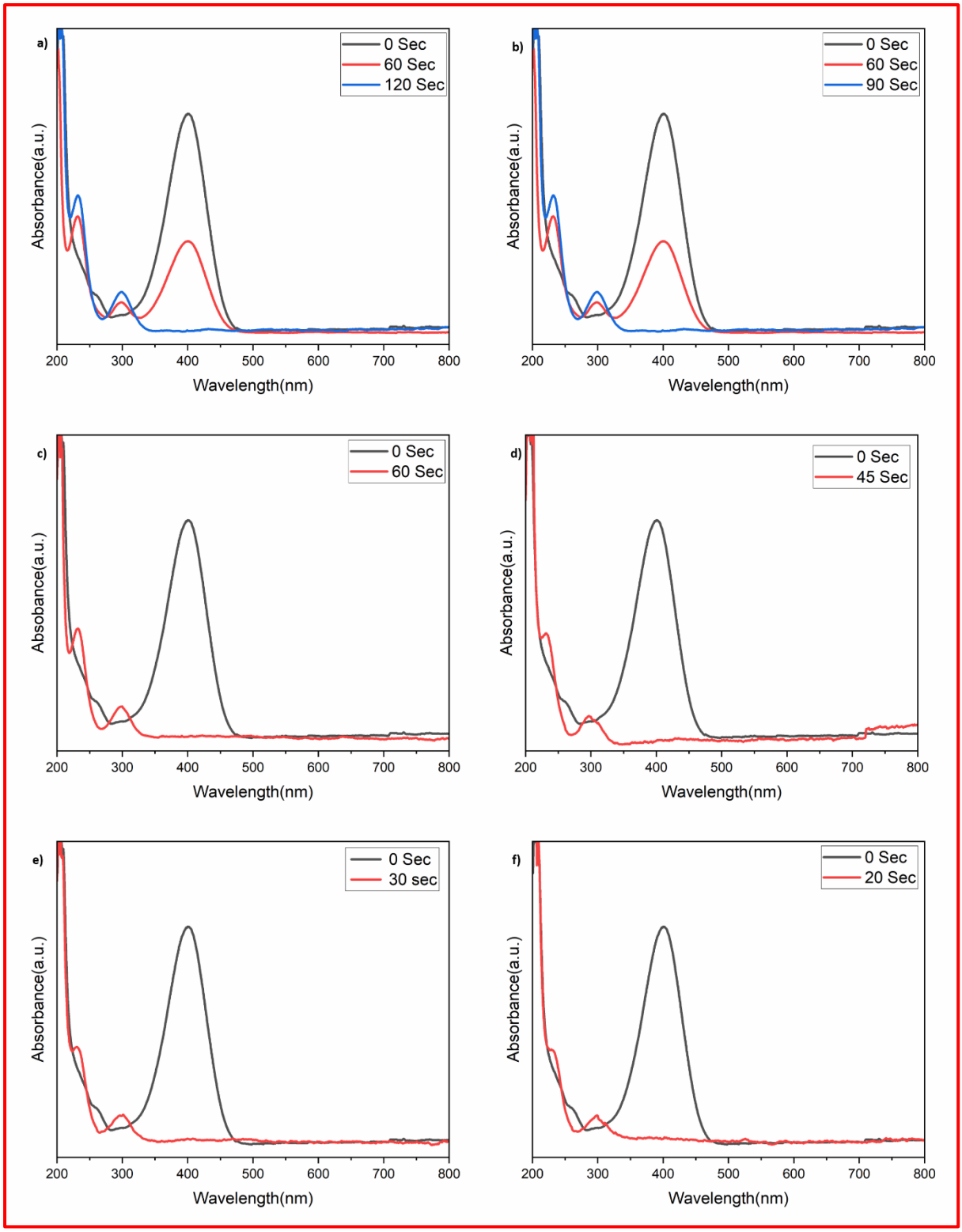

Figure S11. Time-dependent UV–Vis spectra showing the catalytic reduction of 4-nitrophenol to 4-aminophenol using Ag@PBC 500 at different molar ratios of 4-NP:$NaBH_4$: (a) 1:5, (b) 1:10, (c) 1:25, (d) 1:50, (e) 1:75, and (f) 1:100.

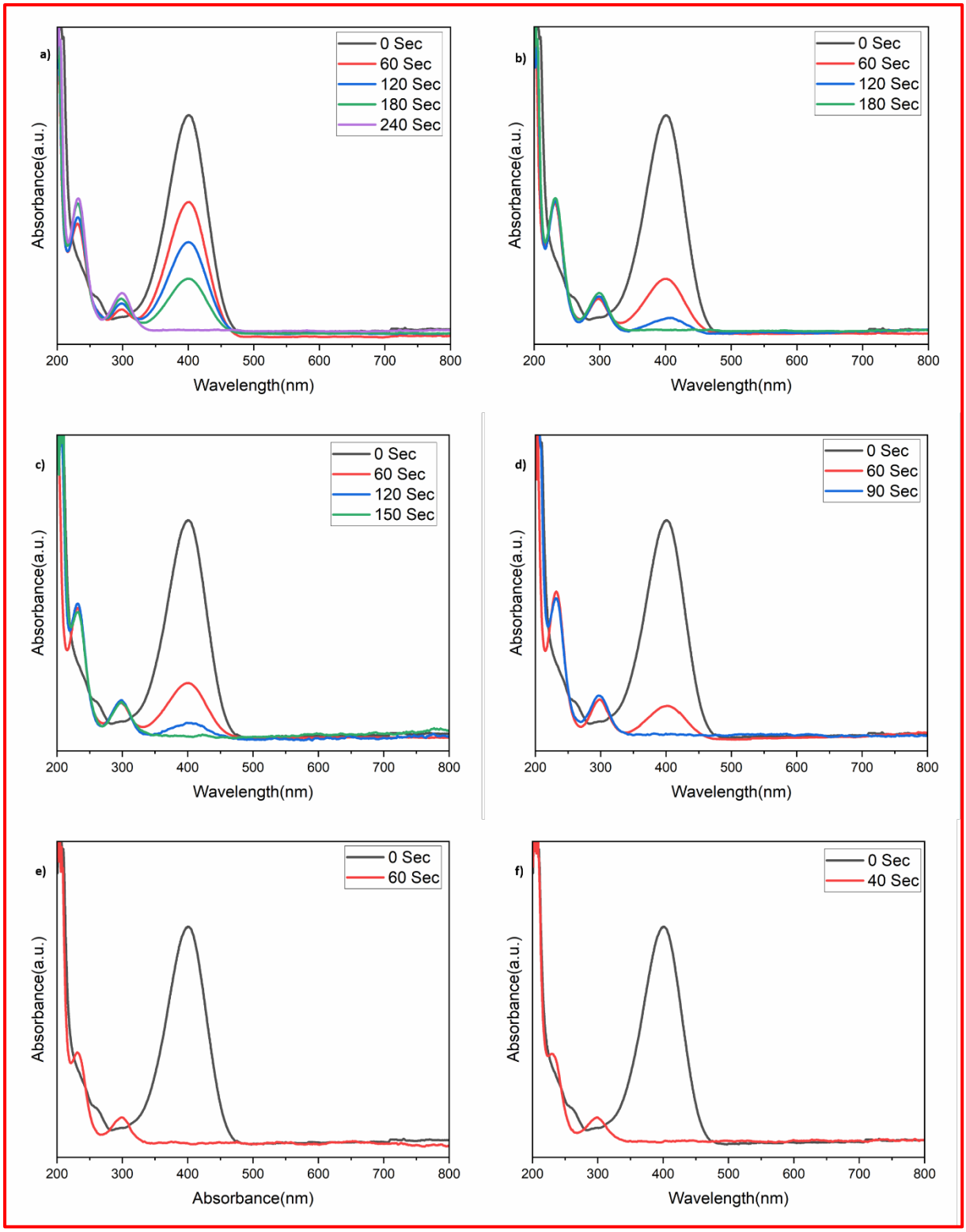

Figure S12. Time-dependent UV–Vis spectra showing the catalytic reduction of 4-nitrophenol to 4-aminophenol using Ag@PBC 600 at different molar ratios of 4-NP:$NaBH_4$: (a) 1:5, (b) 1:10, (c) 1:25, (d) 1:50, (e) 1:75, and (f) 1:100.

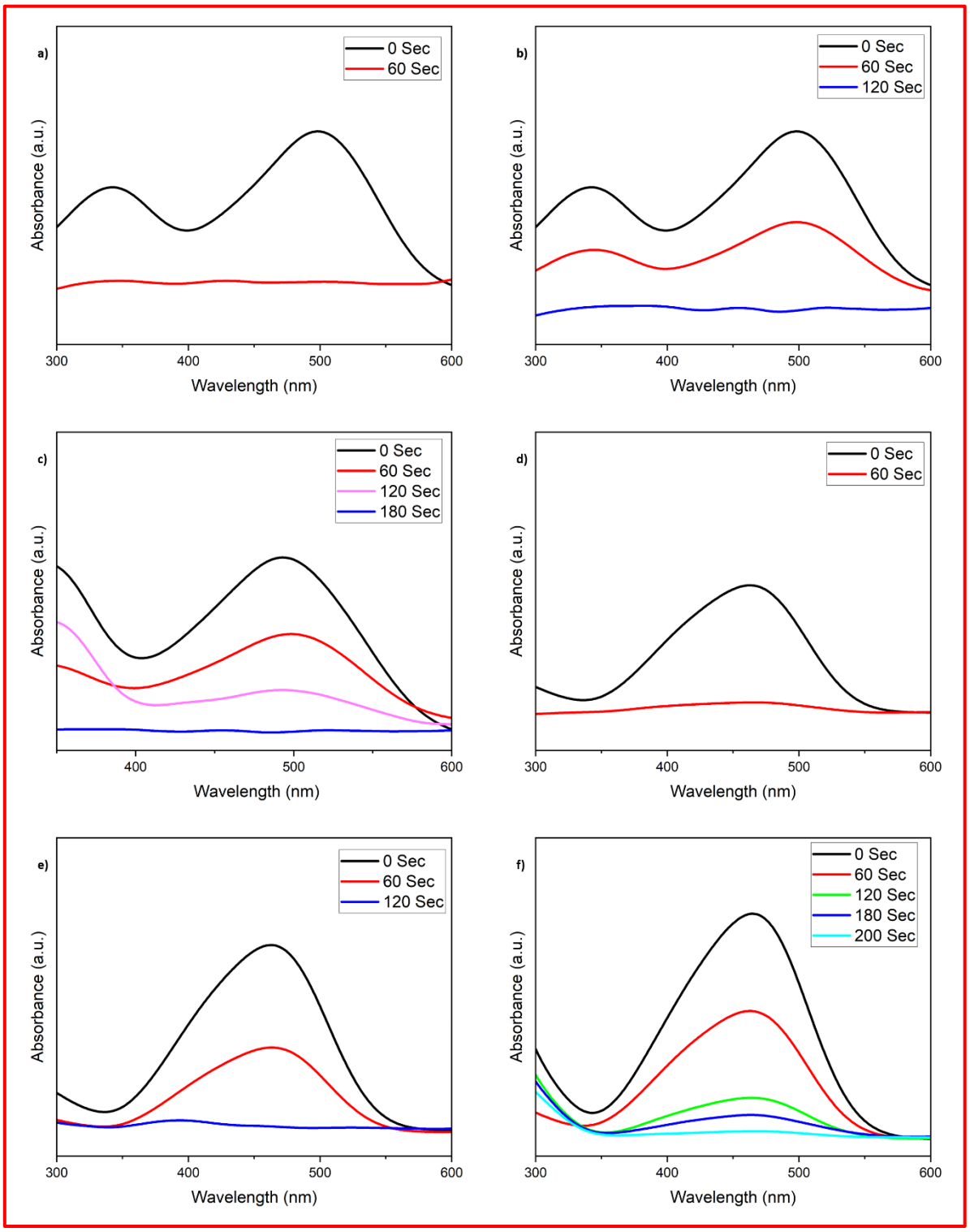

Figure S13. Time-dependent of absorbance showing the reduction of CR and MO at different concentrations 25ppm (a and d), 50ppm (b and e) and 100ppm (c and f) catalyzed by Ag@PBC 300.

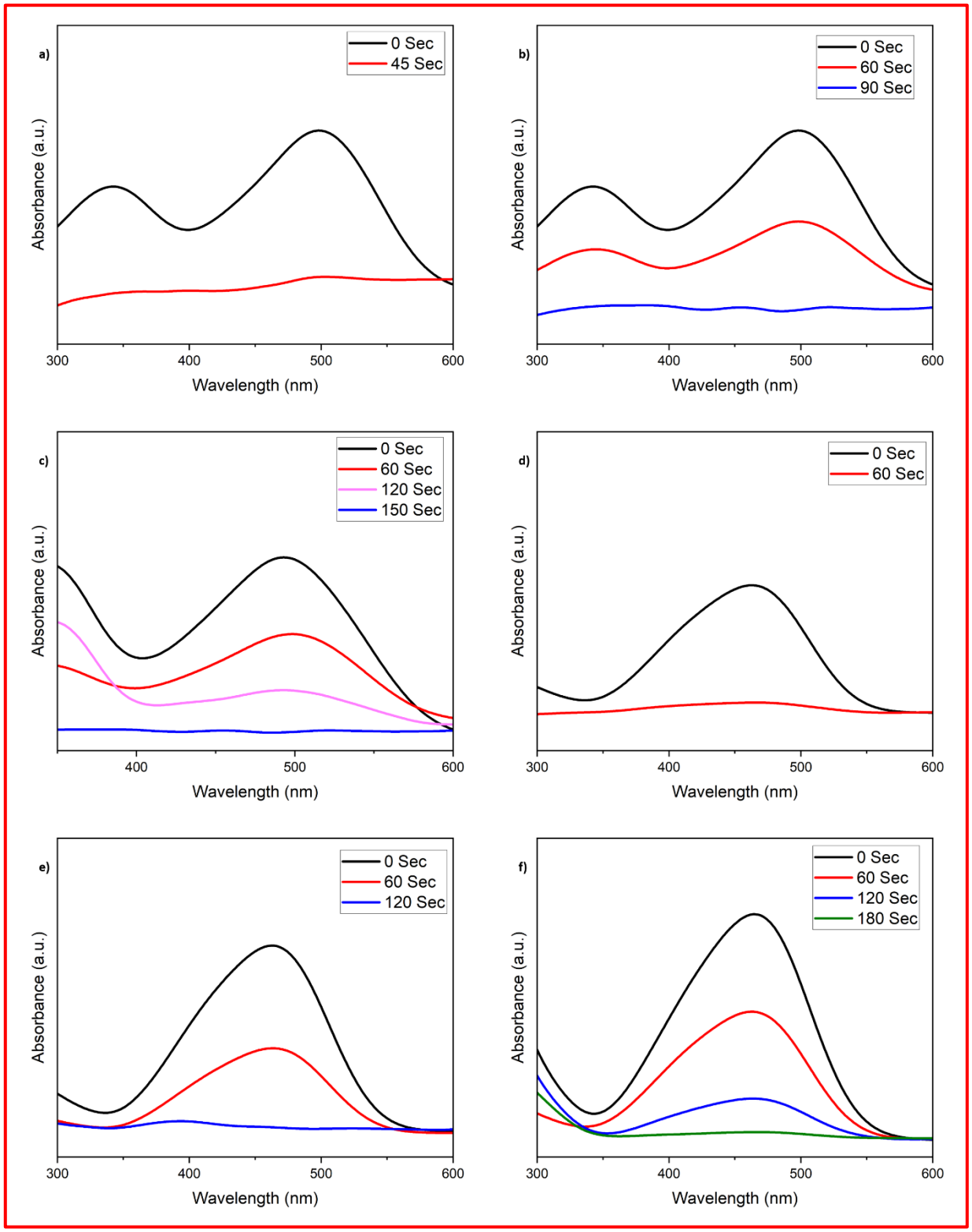

Figure S14. Time-dependent of absorbance showing the reduction of CR and MO at different concentrations 25ppm (a and d), 50ppm (b and e) and 100ppm (c and f) catalyzed by Ag@PBC 400.

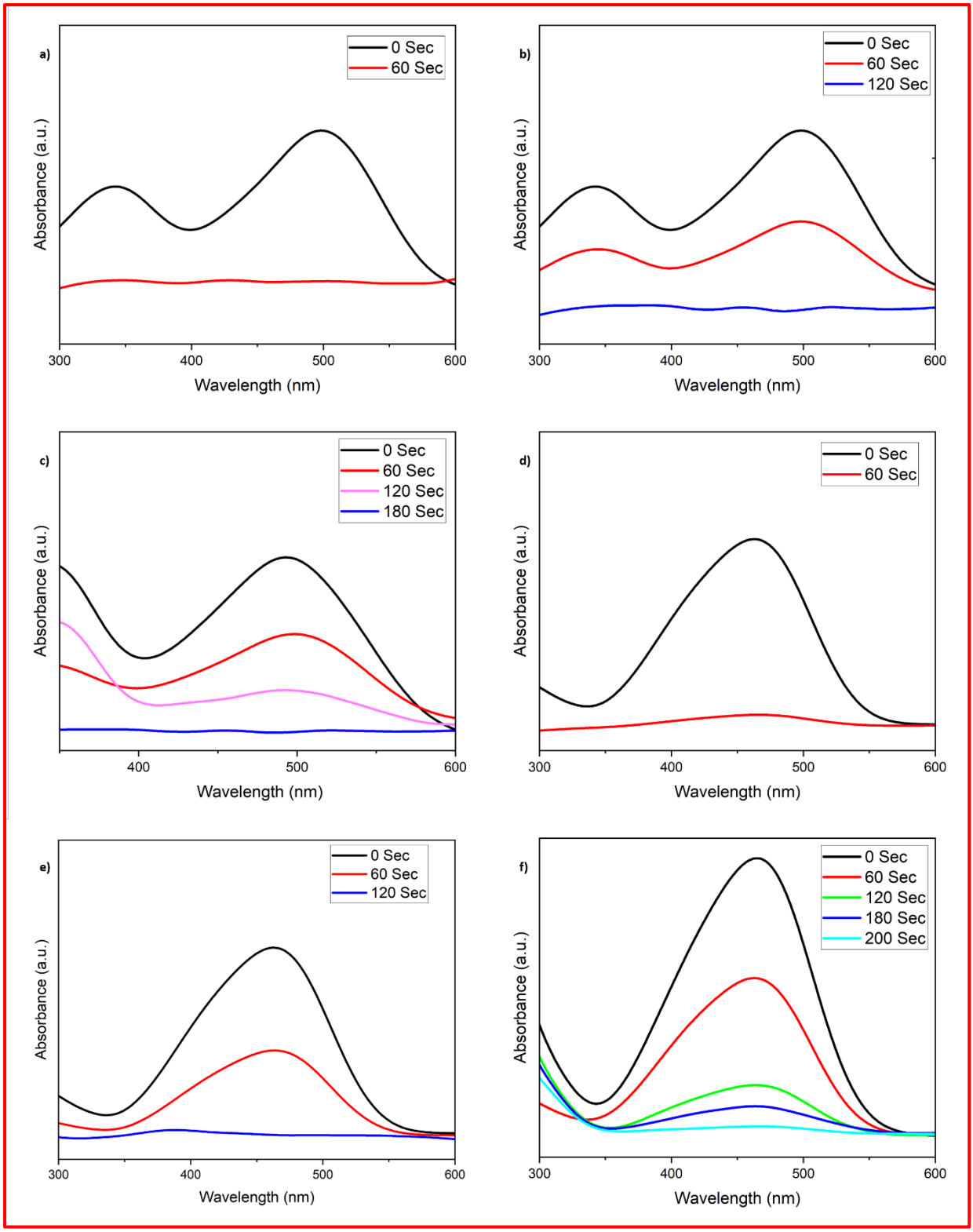

Figure S15. Time-dependent of absorbance showing the reduction of CR and MO at different concentrations 25ppm (a and d), 50ppm (b and e) and 100ppm (c and f) catalyzed by Ag@PBC 600.

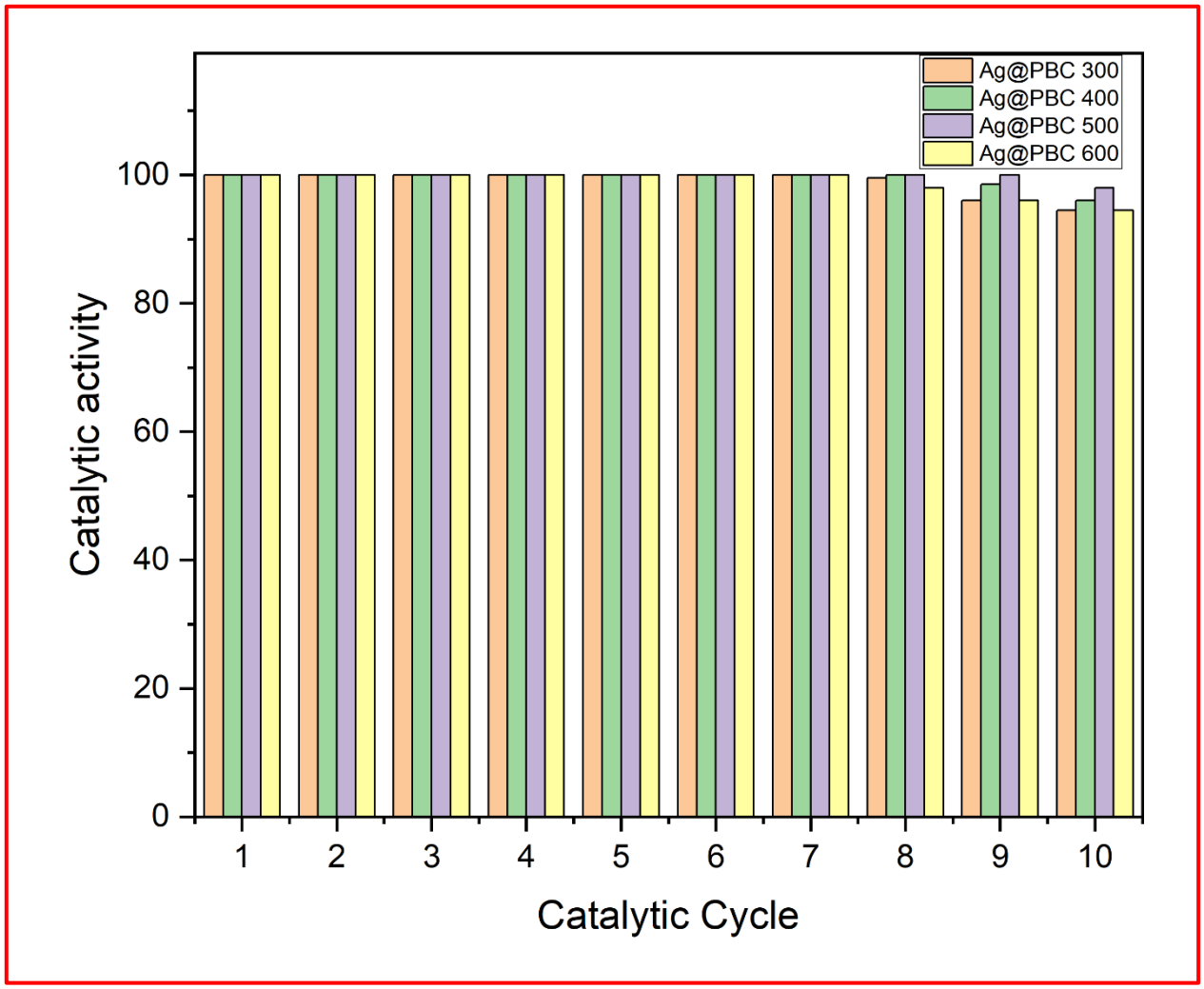

Figure S16. Reusability of Ag@PBC catalysts over 10 cycles.

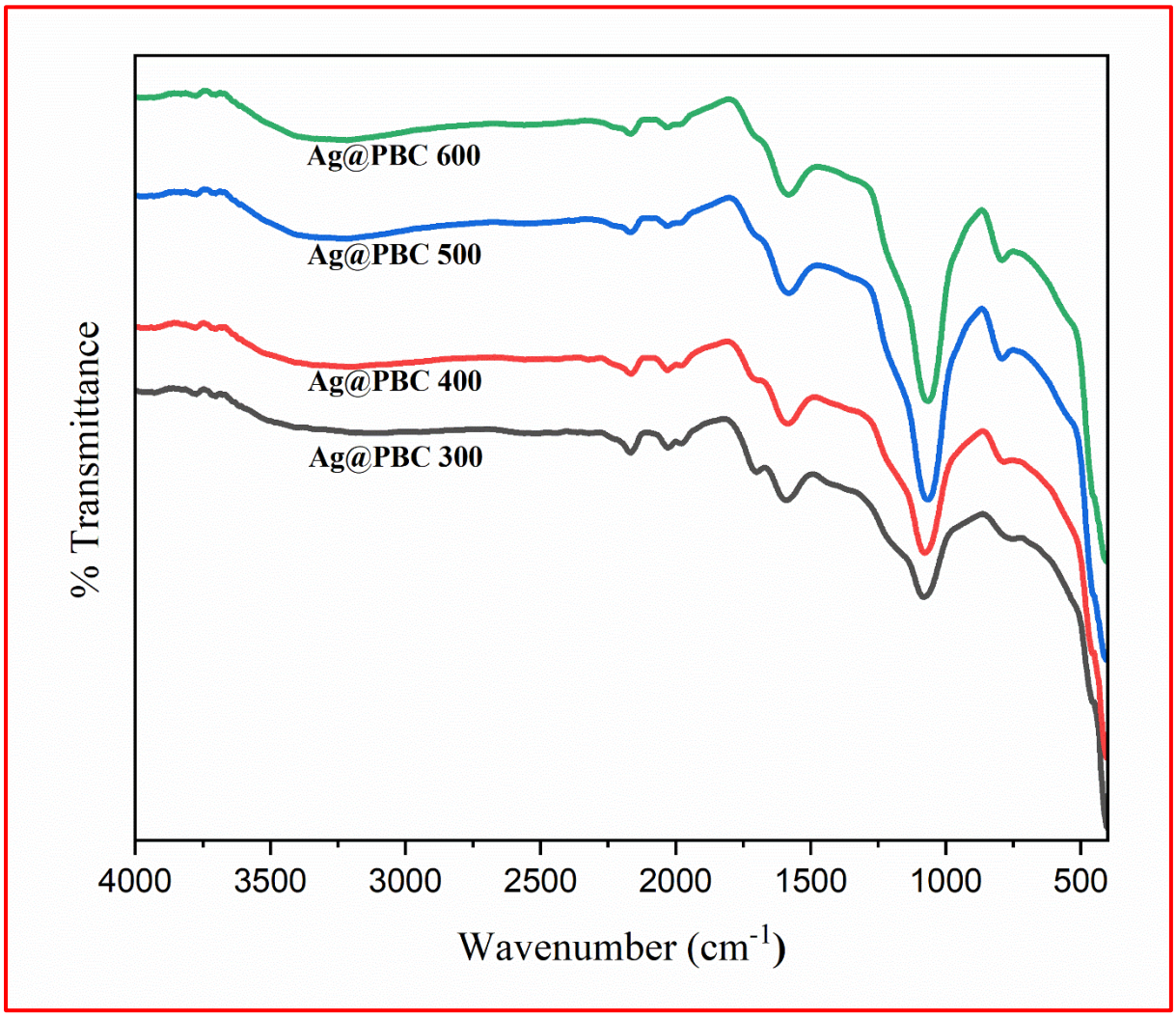

Figure S17. FTIR spectra of the Ag@PBC composites after 10th catalytic cycles.